

**Climatic controls and climate proxy potential of Lewis Glacier, Mt Kenya**

R. Prinz et al.

**Climatic controls and climate proxy potential of Lewis Glacier, Mt Kenya**

R. Prinz<sup>1</sup>, L. I. Nicholson<sup>1</sup>, T. Mölg<sup>2</sup>, W. Gurgiser<sup>1</sup>, and G. Kaser<sup>1</sup>

<sup>1</sup>Institute of Atmospheric and Cryospheric Sciences, University of Innsbruck, Innrain 52, 6020 Innsbruck, Austria

<sup>2</sup>Institute of Geography, Friedrich-Alexander-University Erlangen-Nürnberg (FAU), Wetterkreuz 15, 91058 Erlangen, Germany

Received: 29 May 2015 – Accepted: 29 June 2015 – Published: 28 July 2015

Correspondence to: R. Prinz (rainer.prinz@uibk.ac.at)

Published by Copernicus Publications on behalf of the European Geosciences Union.

Title Page

Abstract

Introduction

Conclusions

References

Tables

Figures



Back

Close

Full Screen / Esc

Printer-friendly Version

Interactive Discussion



## Abstract

The Lewis Glacier on Mt Kenya is one of the best studied tropical glaciers and has experienced considerable retreat since a maximum extent in the late 19th century (L19). From distributed mass and energy balance modelling, this study evaluates the current sensitivity of the surface mass and energy balance to climatic drivers, explores climate conditions under which the L19 maximum extent might have sustained, and discusses the potential for using the glacier retreat to quantify climate change. Multiyear meteorological measurements at 4828 m provide data for input, optimization and evaluation of a spatially distributed glacier mass balance model to quantify the exchanges of energy and mass at the glacier–atmosphere interface. Currently the glacier loses mass due to the imbalance between insufficient accumulation and enhanced melt, because radiative energy gains cannot be compensated by turbulent energy sinks. Exchanging model input data with synthetic climate scenarios, which were sampled from the meteorological measurements and account for coupled climatic variable perturbations, reveal that the current mass balance is most sensitive to changes in atmospheric moisture (via its impact on solid precipitation, cloudiness and surface albedo). Positive mass balances result from scenarios with an increase of annual (seasonal) accumulation of 30% (100%), compared to values observed today, without significant changes in air temperature required. Scenarios with lower air temperatures are drier and associated with lower accumulation and increased net radiation due to reduced cloudiness and albedo. If the scenarios currently producing positive mass balances are applied to the L19 extent, negative mass balances are the result, meaning that the conditions required to sustain the glacier in its L19 extent are not reflected in today’s observations. Alternatively, a balanced mass budget for the L19 extent can be explained by changing model parameters that imply a distinctly different coupling between the glacier’s local surface-air layer and its surrounding boundary-layer. This result underlines the difficulty of deriving paleoclimates for larger glacier extents on the basis of modern measurements of small glaciers.

## Climatic controls and climate proxy potential of Lewis Glacier, Mt Kenya

R. Prinz et al.

Title Page

Abstract

Introduction

Conclusions

References

Tables

Figures



Back

Close

Full Screen / Esc

Printer-friendly Version

Interactive Discussion



# 1 Introduction

Glaciological observations in East Africa over the last century show a pronounced decrease in glacier length, area and mass (Cullen et al., 2013; Hastenrath, 1984, 2005b, 2008; Mölg et al., 2013; Prinz et al., 2011, 2012). Immediate changes in glacier mass are governed by concurrent weather and, consequently by climate through energy and mass exchanges between the glacier surface and the atmosphere. Integrated over time, and filtered by glacier dynamics, these exchanges result in changes in glacier extent. Thus, an accurate understanding of the glacier–climate interaction can be used to reveal the main atmospheric drivers of observed glacier extent changes.

The identification of climate signals from glaciers in East Africa is of particular interest, because they exist in elevations between approximately 5 and 6 km a.s.l. and therefore capture climate signals from the mid-troposphere (Mölg et al., 2009a), where our knowledge of climate change is scarce and controversial (e.g. Hartmann et al., 2013; Karl et al., 2006; Pepin and Lundquist, 2008). The temperature regime of the tropical East African climate – in particular at high elevations – is dominated by a pronounced diurnal cycle, driven by high incoming global radiation during daytime and strong long-wave energy loss during the night (Hastenrath, 1983), resulting in diurnal temperature variations being larger than seasonal temperature variations. The annual cycle is dominated by the hygric seasonality, expressed in the “long rains” (March to May) and the “short rains” (October to December), driven by the passage of the Intertropical Convergence Zone (e.g. Mutai and Ward, 2000) and modulated by Indian Ocean sea surface temperatures (e.g. Yang et al., 2014).

While some initially speculated that glacier recession on Kilimanjaro is caused by rising local air temperature, subsequent physical, process-resolving studies revealed that these glaciers are most sensitive to changes in atmospheric moisture and precipitation (Mölg and Hardy, 2004; Mölg et al., 2008, 2009a) due to their location far above the mean annual freezing level. Although there are additional controls on

TCD

9, 3887–3924, 2015

## Climatic controls and climate proxy potential of Lewis Glacier, Mt Kenya

R. Prinz et al.

Title Page

Abstract

Introduction

Conclusions

References

Tables

Figures



Back

Close

Full Screen / Esc

Printer-friendly Version

Interactive Discussion



## Climatic controls and climate proxy potential of Lewis Glacier, Mt Kenya

R. Prinz et al.

Title Page

Abstract

Introduction

Conclusions

References

Tables

Figures

◀

▶

◀

▶

Back

Close

Full Screen / Esc

Printer-friendly Version

Interactive Discussion



the peculiar plateau icefields (Kaser et al., 2010; Winkler et al., 2010), the ongoing retreat of slope glaciers on Kilimanjaro since the late 19th century is therefore driven by the development of a drier regional atmosphere during the 20th and 21st century (Mölg et al., 2009a). This drying is related to changing ocean conditions which shift the Walker cell circulation over the Indian Ocean, thereby suppressing the convection along the East African continental margin (Chou et al., 2009; Lintner and Neelin, 2007; Mölg et al., 2006; Nicholson, 1996; Tierney et al., 2013; Webster et al., 1999), inhibiting the deep convection required to bring cloud cover and precipitation to the glaciated mountain summit (Mölg et al., 2009c). Both precipitation amount and frequency is reduced, and this combination reduces both the mass additions to the glaciers and the impact of frequent snowfall on surface albedo (Mölg et al., 2009a). The glaciological evidence for a drier atmosphere since the late 19th century is in accordance with alternative proxy climate records that indicate that the decades immediately preceding 1880 were humid, and characterised by high lake stands and relatively abundant precipitation (e.g. Konecky et al., 2014; Nicholson and Yin, 2001; Verschuren et al., 2000).

In contrast to the glaciers on Kilimanjaro, glaciers on Mt Kenya and on Rwenzori exist close to the elevation of the mean regional freezing level, so they can be expected to show more sensitivity to air temperatures than the glaciers of Kilimanjaro. The Lewis Glacier (LG) is the largest glacier on Mt Kenya and has been retreating since the late 19th century. Since 1934 the negative mass balance rate was in line with global estimates of glacier mass balance but since the early 1970s it has been significantly more negative than the global mean (Prinz et al., 2011). Past studies on Mt Kenya used careful assumptions, simple parameterizations and limited meteorological data to attribute the observed retreat of LG to combined changes in radiation geometry, air temperature, precipitation, albedo and cloudiness (Hastenrath and Kruss, 1992; Hastenrath, 2010; Kruss and Hastenrath, 1987, 1990; Kruss, 1983). Although pioneering for their time, data is now available to do a more rigorous assessment of the sensitivity of the glaciers here and explore if, due to their lower

elevation, they offer a different climatic proxy than that offered by the glaciers of Kilimanjaro.

Nicholson et al. (2013) investigated the recent micrometeorological conditions and energy fluxes on LG at the point scale, in the context of other tropical glaciers.

Conditions at the summit of Mt Kenya were found to be much warmer and more humid than on Kilimanjaro, allowing convective clouds to converge over the summit of Mt Kenya much more frequently than over the summit of Kilimanjaro, even though both summits are influenced by the same air masses. The point modelling undertaken by Nicholson et al. (2013) suggests that, unlike on Kilimanjaro, the glacier mass balance variability is not dominated by a single variable or season. Building on that work, this paper aims to (i) extend the point surface energy and mass balance from Nicholson et al. (2013) to glacier wide-values for LG, (ii) evaluate the climate sensitivity of the glacier-wide surface mass and energy balance, (iii) explore climate conditions under which the late 19th century maximum extent of LG might have been sustained and (iv) discuss the potential for using shrinkage of LG to quantify climate change for a time period not covered by instrumental records.

## 2 Data and methods

### 2.1 Study site and in situ meteorological and mass balance observations

Lewis Glacier (0.1 km<sup>2</sup> in 2010) lies ~ 370 m below the summit of Mt Kenya in a south-westerly exposed, quasi-cirque location between the true summit and a secondary peak (Fig. 1). Several authors surveyed LG since 1934 (Prinz et al., 2011 and references therein) and reconstructed the late 19th century maximum extent (L19) from moraines and sketches (Patzelt et al., 1984). The most recent mapping was performed in 2010 (Prinz et al., 2011, 2012) and is used as topographic reference in this paper.

An automatic weather station (AWS) was installed on the glacier surface at an elevation of 4828 m which is ~ 30 m below the upper limit of the glacier. Meteorological

TCD

9, 3887–3924, 2015

## Climatic controls and climate proxy potential of Lewis Glacier, Mt Kenya

R. Prinz et al.

Title Page

Abstract

Introduction

Conclusions

References

Tables

Figures

◀

▶

◀

▶

Back

Close

Full Screen / Esc

Printer-friendly Version

Interactive Discussion





## Climatic controls and climate proxy potential of Lewis Glacier, Mt Kenya

R. Prinz et al.

Title Page

Abstract

Introduction

Conclusions

References

Tables

Figures

◀

▶

◀

▶

Back

Close

Full Screen / Esc

Printer-friendly Version

Interactive Discussion



The model used in this study originates from an energy balance model (Mölg and Hardy, 2004), that was developed into a mass balance model suitable for single point or glacier-wide applications (Mölg et al., 2008, 2009a). The model structure used in this study is explained in detail by Mölg et al. (2012) with the latest model version (2.4) used by Mölg (2015). The model treats the surface and near-subsurface mass and energy fluxes and has been successfully applied to address various questions in a range of climatic conditions (e.g. Collier et al., 2013; Conway and Cullen, 2015; Cullen et al., 2007, 2014; Gurgiser et al., 2013a, b; MacDonell et al., 2013; Mölg et al., 2014; Nicholson et al., 2013). The model computes the mass balance as the sum of solid precipitation, surface deposition, internal accumulation (refreezing of liquid water in snow), change in englacial liquid water storage, subsurface and surface melt, and sublimation. This approach is based on the surface energy balance of a glacier in the following form:

$$SWI(1 - \alpha) + LWI + LWO + QS + QL + QPRC + QC + QPS = F \quad (1)$$

where SWI is incoming shortwave radiation (global radiation corrected for aspect/slope),  $\alpha$  is surface albedo, LWI and LWO are incoming and emitted longwave radiation fluxes, QS and QL are the turbulent fluxes of sensible and latent heat, respectively, QPRC is the heat flux from precipitation, QC the conductive heat flux in the subsurface and QPS the energy flux from shortwave radiation penetrating into the subsurface. The sum of these fluxes yields a residual flux  $F$  which, if the glacier surface temperature (TS) reaches 273.15 K, represents the latent energy for melting. If TS is below 273.15 K, energy conservation is achieved by solving TS to balance the fluxes (Mölg et al., 2009a; van den Broeke et al., 2006). Input data for mass accumulation is provided by a surface height change record or as water equivalent, and SWI,  $\alpha$ , LWI, LWO, air temperature, atmospheric humidity, air pressure and wind speed are required in order to solve the energy balance for the remaining mass fluxes. The model can be validated on the basis of measured surface height changes at the AWS and nearby reference stakes, and/or with TS measured directly or derived from measured

## Climatic controls and climate proxy potential of Lewis Glacier, Mt Kenya

R. Prinz et al.

Title Page

Abstract

Introduction

Conclusions

References

Tables

Figures

◀

▶

◀

▶

Back

Close

Full Screen / Esc

Printer-friendly Version

Interactive Discussion



LWO. In order to enable glacier-wide mass balance runs and sensitivity tests some of these input variables must be replaced by parameterizations based on key atmospheric properties that can then be varied in the sensitivity study. Thus, SWI,  $\alpha$ , LWI are parameterized and TS (LWO) is computed from the energy balance as noted above, to capture the feedback effects on the mass balance in case of a climate perturbation (e.g. Mölg et al., 2009a). The required MBM inputs are therefore reduced to air temperature and humidity, air pressure, a cloud cover factor, wind speed and accumulation rate. Additionally, for the spatially distributed case, a digital elevation model is compulsory as lower boundary condition, from which the grid cell sky view and shading parameters are computed. Vertical gradients in precipitation and air temperature are essential parameters to distribute the meteorological data from the AWS to the whole glacier surface.

### 2.3 Parameterization of radiative fluxes

The MBM's parameterizations for SWI employs the approach from Budyko (1974), which was applied for Equatorial East Africa in earlier studies (Hastenrath, 1984; Mölg et al., 2009b),

$$G = (S_{CS} + D_{CS})(1 - kn_{\text{eff}}), \quad (2)$$

where  $G$  is the global radiation, separated into direct and diffuse clear sky components ( $S_{CS}$  and  $D_{CS}$ ), and  $n_{\text{eff}}$  is the effective cloud cover fraction (0–1). The constant  $k$  controls the global radiation under cloudy conditions. First, clear sky  $G$  is modelled using concepts of Iqbal (1983) and Meyers and Dale (1983) and optimized against measured clear sky days (Mölg et al., 2009b), defined from the meteorological record at the AWS when  $G$  was  $> 77\%$  of top of atmosphere radiation and mean daily longwave net radiation lower than its 5th percentile as a proxy for absent cloudiness (van den Broeke et al., 2006). From 773 days, only 17 clear sky days were found, all occurring in late December to late February. All-sky  $G$  is modelled by optimizing the product  $kn_{\text{eff}}$  over the total measurement period (773 days) and yielding a  $k$  of 0.72,

## Climatic controls and climate proxy potential of Lewis Glacier, Mt Kenya

R. Prinz et al.

Title Page

Abstract

Introduction

Conclusions

References

Tables

Figures

◀

▶

◀

▶

Back

Close

Full Screen / Esc

Printer-friendly Version

Interactive Discussion



meaning that under completely overcast conditions  $G$  is 28 % of its potential clear sky value. Hastenrath (1984) previously used  $k$  of 0.65 for Mt. Kenya based on values from literature and Mölg et al. (2009b) used an optimization based on 700 days of meteorological data to determine that  $k$  is 0.65 for the clearer, drier conditions on the summit of Kilimanjaro (Nicholson et al., 2013). Hence, the higher  $k$  calculated for Mt Kenya is reasonable. Mean daily daytime values of modelled  $G$  correlate highly with measured  $G$  ( $r = 0.99$ ) with a root mean squared error (RMSE) of  $25.4 \text{ W m}^{-2}$  (Fig. 2). Modelling  $G$  outside the calibration period (872 days of AWS on Radio Ridge) yielded very similar statistics ( $r = 0.99$  and RMSE of  $27.0 \text{ W m}^{-2}$ ), indicating that despite the limited number of clear sky days available for model optimization the parameterization scheme is robust.

LWI is described by the Stefan–Boltzmann law and depends on the atmospheric emissivity ( $\varepsilon_A$ ), the Stefan–Boltzmann constant ( $\sigma$ ) and the absolute temperature of the air. The presence of clouds increases  $\varepsilon_A$  by a cloud factor  $F_{cl}$  ( $\geq 1$ ), which is thus positively correlated with  $n_{eff}$  (Niemelä et al., 2001) and can be written as the ratio of all sky LWI/clear sky LWI (Mölg et al., 2009b; Sicart et al., 2006).

$$LWI = \varepsilon_{ACS} \sigma T^4 F_{cl} \quad (3)$$

For clear sky LWI, the clear sky atmospheric emissivity ( $\varepsilon_{ACS}$ ) was derived optimizing the constants  $c1$  (1.24) and  $c2$  (7.6) in an empiric relationship from Brutsaert (1975),

$$\varepsilon_{ACS} = c1 \left( \frac{e}{T} \right)^{\frac{1}{c2}} \quad (4)$$

where  $e$  is the atmospheric vapour pressure and  $T$  the absolute air temperature. Finally, all sky LWI is modelled finding an optimal function  $F_{cl}(n_{eff})$ . Mean daily values of modelled LWI correlate to measured LWI with  $r = 0.95$  at a RMSE of  $8.3 \text{ W m}^{-2}$  (Fig. 2).

$$F_{cl} = \frac{LWI_{all\ sky}}{LWI_{clear\ sky}} = -0.316n_{eff}^3 + 0.2697n_{eff}^2 + 0.39773n_{eff} + 0.97119 \quad (5)$$

To account for long wave irradiance from surrounding terrain LWI in the distributed MBM runs was finally computed as,

$$LWI = s_f LWI_{sky} + (1 - s_f) \varepsilon_R \sigma T_R^4 \quad (6)$$

where  $LWI_{sky}$  is the long wave irradiance from the sky (Eq. 3),  $s_f$  the sky view factor,  $\varepsilon_R$  the terrain emissivity (0.98) and  $T_R$  the terrain temperature (absolute air temperature + 0.01  $KW^{-1} m^2 G$ ), the latter being found less sensitive than  $s_f$  in steep topography of low latitudes (Sicart et al., 2006, 2011).

The parameterization of  $\alpha$  (Fig. 3) is a function of snow fall frequency, time since the last snow fall and snow depth (Oerlemans and Knap, 1998). The parameterization retains  $\alpha$  of underlying snow, in case this layer becomes re-exposed after melting of new snow above (Gurgiser et al., 2013b; Mölg et al., 2012). The effects of snow ageing and snow depth on  $\alpha$  are given by e-folding constants to compute values for  $\alpha$  between constant fresh snow and firn albedos and variable ice albedo ( $\alpha_{ice}$ ), which is a function of the dew point temperature (Fig. 3). Hence,  $\alpha_{ice}$  is adapted to tropical conditions, where ablation processes (melt or sublimation) strongly impact  $\alpha_{ice}$  (Corripio and Purves, 2005; Mölg et al., 2008; Winkler et al., 2009).

## 2.4 Model optimization and uncertainty estimation at the AWS

Model parameter sensitivities to mass balance were estimated with the same MBM for different climate settings in classical single-parameter variations (Mölg et al., 2009a) or multi-parameter variations through Monte Carlo approaches (Gurgiser et al., 2013b; Mölg et al., 2012). For LG Nicholson et al. (2013) adopted the Monte Carlo approach to optimize the model parameters for the available periods of measured meteorological input at the point of the AWS and evaluated the model performance against independent stake measurements. However, this does not provide an estimate of the model performance outside the period of optimization, which is an inadequate error assessment for sensitivity studies that involve forcing the model with perturbed

Title Page

Abstract

Introduction

Conclusions

References

Tables

Figures

◀

▶

◀

▶

Back

Close

Full Screen / Esc

Printer-friendly Version

Interactive Discussion







## Climatic controls and climate proxy potential of Lewis Glacier, Mt Kenya

R. Prinz et al.

Title Page

Abstract

Introduction

Conclusions

References

Tables

Figures

◀

▶

◀

▶

Back

Close

Full Screen / Esc

Printer-friendly Version

Interactive Discussion



do not allow for a quantified partitioning of potential dynamic processes causing strong daytime gradients observed at the margins of glaciers (Ayala et al., 2015; Carturan et al., 2015; Petersen and Pellicciotti, 2011), the daytime gradient of  $-0.015^{\circ}\text{C m}^{-1}$  was found through optimization using the spatially distributed stake mass balances of 2011/12. As the component of LWI that is parameterized for terrestrial irradiance from the surroundings is not constrained by measurements, the optimized daytime vertical air temperature gradient will also compensate for shortcomings in the LWI parameterization. LG spans only 220 m in altitude, so the mean nocturnal and diurnal air temperature differences from the top (measured) to the terminus of the glacier (from the optimized vertical air temperature gradient extrapolations) are 1.4 and  $3.3^{\circ}\text{C}$  respectively.

### 2.6 Sampling synthetic climate scenarios

As described by Nicholson et al. (2013) it is unlikely that a single climatic variable dominates the mass balance variability on LG. Thus, exploring mass balance sensitivity of single climatic variable perturbation was rejected in favour of coupled perturbations reflecting the variability in the climate more comprehensively (Mölg et al., 2009a). Consequently, in order to assess the sensitivity of the mass balance to a perturbation in its forcing climate, alternative climate scenarios were constructed by reassembling the AWS records on a diurnal basis in a very simple, weather generator like concept (e.g. Hutchinson, 1987). The period of AWS data has been shown to be representative for the recent decades in terms of monthly ERA-interim air temperature (1979–2012) and TRMM precipitation (1998–2012) time series (Fig. 3 in Nicholson et al., 2013). Out of the 773 days with meteorological data from LG AWS, 365 days (representing one arbitrary mass balance year from 1 March to 28 February) were sampled with replacement to construct four differently perturbed, synthetic climate scenarios meeting the following characteristics compared to the 2011/12 REF year: +1 K air temperature (warm and wet, WW), -1 K air temperature (cold and dry, CD), +50 % accumulation (WET), and -20 % accumulation (DRY). To maintain the actual hygric seasonality, the

selected days were sorted for accumulation with the wettest (driest) days randomly assigned to the wet (dry) seasons, minus one week to smooth the transitions between them. As there is insignificant seasonality in air temperature in this inner-tropical setting (Hastenrath, 1983), forced assignation of the annual temperature variations was neglected.

High interannual variability in East African precipitation seasonality is characteristic for this region as droughts can occur and/or prolong into wet seasons and exchange with periods of above normal precipitation, which has been observed in recent decades (e.g. Black et al., 2003; Nicholson, 2015). To cover the interannual variability, three further scenarios were constructed to explore the impact of potentially varying amplitudes of seasonal cycles: A warm amplification (AMPW) in which the wet seasons from WW and the dry seasons from CD are merged, a cold amplification (AMPC) in which the wet seasons from WET and the dry seasons from CD are merged, and an attenuated scenario (ATT) in which the wet seasons from CD are combined with the dry seasons from WW. Table 4 lists annual and seasonal statistics for all seven scenarios and the 2011/12 reference climate. This way a set of physically consistent and complex climate perturbations was obtained. Incoming radiative fluxes are parametrized from these resampled inputs as explained in Sect. 2.3. In the absence of any data, the 1 K perturbation for air temperature was chosen arbitrarily, but the perturbation in accumulation reflects measured precipitation variation at Austrian Hut between 1978 and 1996 (Hastenrath, 2005a). They show an annual minimum/mean/maximum) of 480/850/1300 mm. Cumulative annual accumulation (i.e. snow depth in cm) from the scenarios converted with a fresh snow density of  $315 \text{ kg m}^{-3}$  (Table 2) yield annual precipitation sums between 480 mm (CD), 731 mm (REF) and 1120 mm (WW), which are in the range of previously reported values.

## Climatic controls and climate proxy potential of Lewis Glacier, Mt Kenya

R. Prinz et al.

Title Page

Abstract

Introduction

Conclusions

References

Tables

Figures

◀

▶

◀

▶

Back

Close

Full Screen / Esc

Printer-friendly Version

Interactive Discussion



### 3 Results and discussion

#### 3.1 The mass and energy balance for the year 2011/12

Modelled annual mass balance at the 23 ablation stakes available for 2011/12 is significantly correlated to the measured mass balance with  $r = 0.86$  at an RSME of  $320 \text{ kg m}^{-2}$  (Fig. 4). Propagating the combined errors of the cross validation and comparison to the measured mass balance at all stakes, the modelled glacier mass balance for 2011/12 is  $-911 \pm 355 \text{ kg m}^{-2}$ , which agrees well with the measured value<sup>1</sup> of  $-961 \text{ kg m}^{-2}$ . The model sensitivity of the mass balance to the vertical air temperature gradient is  $-20 \text{ kg m}^{-2}$  for each increase of  $0.001 \text{ }^\circ\text{C m}^{-1}$  (between  $-0.015$  and  $-0.0065 \text{ }^\circ\text{C m}^{-1}$ ) and  $6 \text{ kg m}^{-2}$  for each increase of the vertical precipitation gradient of  $0.001 \text{ } \%$   $\text{m}^{-1}$  (between  $-0.005$  and  $-0.01 \text{ } \%$   $\text{m}^{-1}$ ).

Glacier-wide mean monthly energy and mass flux densities for 2011/12 are shown in Fig. 5. The governing role of the net short-wave flux on the energy and mass balance is clear. When  $\alpha$  is high, due to abundant snow accumulation, the energy available for ablation is reduced, enabling conditions for net accumulation. In contrast, during the January/February dry season increased net radiation and turbulent fluxes cause high ablation rates. Both long-wave fluxes are almost constant throughout the year, as a potential lower LWI in colder and drier conditions is compensated by increased emission from surrounding terrain due to its enhanced solar heating, and TS reaches regularly  $0 \text{ }^\circ\text{C}$ . The seasonal cycle in 2011/12 is attenuated in the first half of the record and amplified in the latter, due to accumulation amounts below normal in the “long rains” and above normal in the “short rains”, respectively (Nicholson et al., 2013).

<sup>1</sup>For the mass balance year 2011/12 Prinz et al. (2012) reported an annual mass balance of  $-1030 \text{ kg m}^{-2}$ . This value changed to  $-961 \text{ kg m}^{-2}$  as the spatial interpolation of observed mass change from the ablation stakes to the glacier area was homogenized by using contours with constant equidistance.

Title Page

Abstract

Introduction

Conclusions

References

Tables

Figures

◀

▶

◀

▶

Back

Close

Full Screen / Esc

Printer-friendly Version

Interactive Discussion







## Climatic controls and climate proxy potential of Lewis Glacier, Mt Kenya

R. Prinz et al.

Title Page

Abstract

Introduction

Conclusions

References

Tables

Figures

⏪

⏩

◀

▶

Back

Close

Full Screen / Esc

Printer-friendly Version

Interactive Discussion



the air above is maintained due to effective long-wave surface cooling and energy consumption by QL, and higher wind speeds enhance both turbulent fluxes. Thus, the physically-based modelling study presented here indicates that for climate scenarios that are within the limits of observations, only a change in the mountain's precipitation climatology to substantially more accumulation is able to sustain LG in its current extent.

### 3.3 Modelling and interpreting L19 mass balance

The mass balance model was applied to the LG in its L19 extent with the two most positive mass balance scenarios synthesized from the range of observed modern climate conditions (scenarios WET and AMPC) to see if these perturbed climates are sufficient to sustain the L19 glacier extent. The modelling produced negative mass balances in both cases of  $-233 \text{ kg m}^{-2}$  (WET) and  $-338 \text{ kg m}^{-2}$  (AMPC), respectively. Again, in these simulations, the impact of the strong air temperature gradient on the phase change of precipitation over the L19 extent is minor and confined to the lowest parts ( $< 4550 \text{ m}$ ), where the maximum reduction of accumulation in favour of rain is 13% for the lowest grid point. Over the total glacier area the fraction of rain is less than 1% for both scenarios WET and AMPC.

The negative mass balances for these scenarios, being most favourable to glaciation, imply that even the extremes of the present day climate are incapable of reproducing the L19 conditions. One interpretation of this finding is that the range of modern-day meteorological conditions in the summit region of Mt Kenya no longer overlaps with the L19 range, and/or the covariance of meteorological conditions was substantially different in L19 than today.

### 3.4 The impact of glacier extent on the proxy potential of Lewis Glacier

Given that LG is now 83% smaller than its L19 extent, the relative importance of the glacier microclimate relative to the surrounding terrain is likely to have changed

significantly between these two glacier geometries (Fig. 1). The limited aerial and vertical extent of the modern glacier favours the steep vertical air temperature gradient along the glacier surface, but on larger glaciers such as LG during its L19 extent, the air temperature gradient over the glacier surface is strongly modified by the katabatic wind field (Ayala et al., 2015; Greuell and Böhm, 1998; Shea and Moore, 2010), and the influence of longwave emissions from surrounding terrain is drastically reduced as the glacier fills the cirque (Fig. 1).

Given the small area of LG in the modern day, it could be that the glacier is too small to form a substantial katabatic layer and modify its own microclimate and is instead more strongly influenced by the surroundings with the off-glacier boundary layer conditions dominating over much of the lower glacier. If this is the case, the air temperature distribution optimized for the modern-day LG extent cannot capture the dynamic processes that play a part in governing the air temperature distribution over the larger L19 glacier extent. Repeating the modelling for the L19 glacier extent using the moist adiabatic lapse rate for all hours of the day gives mass balances of 190 and 68 kg m<sup>-2</sup> for WET and AMPC respectively, and quasi-zero mass balances (17, -2 kg m<sup>-2</sup>, for WET and AMPC respectively) can be achieved by using daytime vertical air temperature gradients of -0.010 and -0.008 °C m<sup>-1</sup>, respectively. This supports the idea that a larger glacier can develop a deeper katabatic boundary layer that is more difficult to entrain through advection and turbulent mixing of warm air. Thus, reconstructions of former or future climates that are based on model optimizations for a modern-day glacier extent may not be applicable to substantially different glacier extents. This might have particular relevance for reconstructions based on very small glaciers such as LG, especially when glacier geometries changed significantly. Ongoing retreat of remaining mountain glaciers suggests that scale effects such as this might also become increasingly important for paleoclimate reconstructions from mountain glaciers in the future.

## Climatic controls and climate proxy potential of Lewis Glacier, Mt Kenya

R. Prinz et al.

Title Page

Abstract

Introduction

Conclusions

References

Tables

Figures

◀

▶

◀

▶

Back

Close

Full Screen / Esc

Printer-friendly Version

Interactive Discussion



## 4 Conclusion

Distributed surface energy and mass balance modelling indicates that the energy and mass balance of present-day Lewis Glacier is most sensitive to atmospheric moisture (solid precipitation, cloudiness and albedo). In the tropical atmosphere of Mount Kenya, air temperature changes are always coexistent with changes in atmospheric moisture; consequently, air temperature variation cannot be isolated as a single driver of glacier mass change. Although it has been proposed that a reduction in air temperature of  $0.7^{\circ}\text{C}$  would be sufficient to bring this small glacier to a zero mass balance state (Hastenrath, 2010), a colder climate scenario results in a less negative mass balance, but without additional accumulation it is insufficient to achieve equilibrium.

Two scenarios suggest that higher accumulation ( $+30$  to  $+100\%$  year $^{-1}$  or wet season, respectively), higher relative humidity (4 to 8% units per year or dry season), a change of fractional cloud cover ( $-5$  to  $+1\%$  units per dry season or year) and higher wind speed ( $0.3$  to  $0.6\text{ ms}^{-1}$  year $^{-1}$  or dry season), which are all mutually linked, allow a zero mass balance for the present day Lewis Glacier, without significant changes in the air temperature.

Using the mass balance model as optimized for the modern-day glacier, driven by climate perturbations reflecting the observed variability in precipitation and air temperature, indicates that L19 conditions at LG were distinctly different to the present day, and it is not possible to fully quantify the climatic conditions that could sustain LG at its maximum L19 extent. Additionally, the modelling suggests that extracting proxy climate conditions from a particular glacier geometry using a modelling system optimized on a dramatically different geometry may invalidate the approach, particularly if changes in boundary layer dynamics are substantial and not resolved in the model. This issue might warrant further investigation given that paleoclimate reconstructions based on mountain glacier fluctuations inherently involve these scale contrasts, yet they are rarely considered in the tools used.



## Climatic controls and climate proxy potential of Lewis Glacier, Mt Kenya

R. Prinz et al.

Title Page

Abstract

Introduction

Conclusions

References

Tables

Figures

◀

▶

◀

▶

Back

Close

Full Screen / Esc

Printer-friendly Version

Interactive Discussion



Brock, B. W., Willis, I. C., and Sharp, M. J.: Measurement and parameterization of aerodynamic roughness length variations at Haut Glacier d'Arolla, Switzerland, *J. Glaciol.*, 52, 281–297, doi:10.3189/172756506781828746, 2006.

Brutsaert, W.: On a derivable formula for long-wave radiation from clear skies, *Water Resour. Res.*, 11, 742–744, 1975.

Budyko, M. I.: *Climate and Life*, Academic Press, New York and London, 1974.

Carturan, L., Cazorzi, F., De Blasi, F., and Dalla Fontana, G.: Air temperature variability over three glaciers in the Ortles–Cevedale (Italian Alps): effects of glacier fragmentation, comparison of calculation methods, and impacts on mass balance modeling, *The Cryosphere*, 9, 1129–1146, doi:10.5194/tc-9-1129-2015, 2015.

Charnley, F. E.: Some observations on the glaciers of Mount Kenya, *J. Glaciol.*, 3, 483–492, 1959.

Chou, C. and Neelin, J. D.: Mechanisms of global warming impacts on robustness of tropical precipitation asymmetry, *J. Climate*, 17, 2688–2701, doi:10.1175/1520-0442(2004)017<2688:MOGWIO>2.0.CO;2, 2004.

Chou, C., Neelin, J. D., Chen, C. A., and Tu, J. Y.: Evaluating the “rich-get-richer” mechanism in tropical precipitation change under global warming, *J. Climate*, 22, 1982–2005, doi:10.1175/2008JCLI2471.1, 2009.

Collier, E., Mölg, T., Maussion, F., Scherer, D., Mayer, C., and Bush, A. B. G.: High-resolution interactive modelling of the mountain glacier–atmosphere interface: an application over the Karakoram, *The Cryosphere*, 7, 779–795, doi:10.5194/tc-7-779-2013, 2013.

Conway, J. P. and Cullen, N. J.: Cloud effects on the surface energy and mass balance of Brewster Glacier, New Zealand, *The Cryosphere Discuss.*, 9, 975–1019, doi:10.5194/tcd-9-975-2015, 2015.

Corripio, J. G. and Purves, R. S.: Surface energy balance of high altitude glaciers in the Central Andes: the effect of snow penitentes, in: *Climate and Hydrology in Mountain Areas*, edited by: de Jong, C., Collins, D., and Ranzi, R., John Wiley & Sons, Ltd, Chichester, 15–27, 2005.

Cullen, N. J., Mölg, T., Kaser, G., Steffen, K., and Hardy, D. R.: Energy-balance model validation on the top of Kilimanjaro, Tanzania, using eddy covariance data, *Ann. Glaciol.*, 46, 227–233, doi:10.3189/172756407782871224, 2007.

Cullen, N. J., Sirguey, P., Mölg, T., Kaser, G., Winkler, M., and Fitzsimons, S. J.: A century of ice retreat on Kilimanjaro: the mapping reloaded, *The Cryosphere*, 7, 419–431, doi:10.5194/tc-7-419-2013, 2013.



## Climatic controls and climate proxy potential of Lewis Glacier, Mt Kenya

R. Prinz et al.

Title Page

Abstract

Introduction

Conclusions

References

Tables

Figures

◀

▶

◀

▶

Back

Close

Full Screen / Esc

Printer-friendly Version

Interactive Discussion



- Hastenrath, S.: Glaciological Studies on Mount Kenya, University of Wisconsin-Madison, Madison, 2005a.
- Hastenrath, S.: The glaciers of Mount Kenya 1899–2004, *Erdkunde*, 59, 120–125, doi:10.3112/erdkunde.2005.02.03, 2005b.
- 5 Hastenrath, S.: Recession of Equatorial Glaciers: a Photo Documentation, Sundog, Madison, 2008.
- Hastenrath, S.: Climatic forcing of glacier thinning on the mountains of equatorial East Africa, *Int. J. Climatol.*, 30, 146–152, doi:10.1002/joc.1866, 2010.
- Hastenrath, S. and Kruss, P. D.: Greenhouse indicators in Kenya, *Nature*, 335, 503–504, 1992.
- 10 Hutchinson, M. F.: Methods of generation of weather sequences, in: *Agricultural Environments: Characterization, Classification and Mapping*, edited by: Bunting, A. H., CAB International, Wallingford, UK, 149–157, 1987.
- Iqbal, M.: *An Introduction to Solar Radiation*, Academic Press Canada, Toronto, 1983.
- Karl, T. R., Hassol, S. J., Miller, C. D., and Murray, W. L.: *Temperature Trends in the Lower Atmosphere: Steps for Understanding and Reconciling Differences*, General Books LLC, Washington, DC, 2006.
- 15 Kaser, G., Georges, C., Juen, I., and Mölg, T.: Low-latitude glaciers: unique global climate indicators and essential contributors to regional fresh water supply. A conceptual approach, in: *Global Change and Mountain Regions: An Overview of Current Knowledge*, edited by: Huber, U., Bugmann, H. K. M., and Reasoner, M. A., Kluwer, New York, 185–196, 2005.
- 20 Kaser, G., Mölg, T., Cullen, N. J., Hardy, D. R., and Winkler, M.: Is the decline of ice on Kilimanjaro unprecedented in the Holocene?, *Holocene*, 20, 1079–1091, doi:10.1177/0959683610369498, 2010.
- Konecky, B., Russell, J., Huang, Y., Vuille, M., Cohen, L., and Street-Perrott, F. A.: Impact of monsoons, temperature, and CO<sub>2</sub> on the rainfall and ecosystems of Mt. Kenya during the Common Era, *Palaeogeogr. Palaeoclimatol.*, 396, 17–25, doi:10.1016/j.palaeo.2013.12.037, 2014.
- 25 Kruss, P. D.: Climate change in east Africa: a numerical simulation from the 100 years of terminus record at Lewis Glacier, Mount Kenya, Kenya, *Zeitschrift für Gletscherkunde und Glazialgeologie*, 19, 43–60, 1983.
- 30 Kruss, P. D. and Hastenrath, S.: The role of radiation geometry in the climate response of Mount Kenya's glaciers, Part 1: Horizontal reference surfaces, *Int. J. Climatol.*, 7, 493–505, doi:10.1002/joc.3370070505, 1987.

## Climatic controls and climate proxy potential of Lewis Glacier, Mt Kenya

R. Prinz et al.

Title Page

Abstract

Introduction

Conclusions

References

Tables

Figures

◀

▶

◀

▶

Back

Close

Full Screen / Esc

Printer-friendly Version

Interactive Discussion



Kruss, P. D. and Hastenrath, S.: The role of radiation geometry in the climate response of Mount Kenya's glaciers, Part 3: The latitude effect, *Int. J. Climatol.*, 10, 321–328, doi:10.1002/joc.3370100309, 1990.

Lintner, B. R. and Neelin, J. D.: A prototype for convective margin shifts, *Geophys. Res. Lett.*, 34, L05812, doi:10.1029/2006GL027305, 2007.

MacDonell, S., Kinnard, C., Mölg, T., Nicholson, L., and Abermann, J.: Meteorological drivers of ablation processes on a cold glacier in the semi-arid Andes of Chile, *The Cryosphere*, 7, 1513–1526, doi:10.5194/tc-7-1513-2013, 2013.

Meyers, T. P. and Dale, R. F.: Predicting daily insolation with hourly cloud height and coverage, *J. Clim. Appl. Meteorol.*, 22, 537–545, 1983.

Mölg, T.: Exploring the concept of maximum entropy production for the local atmosphere-glacier system, *J. Adv. Model. Earth Syst.*, 7, 1–11, doi:10.1002/2014MS000404, 2015.

Mölg, T. and Hardy, D. R.: Ablation and associated energy balance of a horizontal glacier surface on Kilimanjaro, *J. Geophys. Res.*, 109, D16104, doi:10.1029/2003JD004338, 2004.

Mölg, T., Renold, M., Vuille, M., Cullen, N. J., Stocker, T. F., and Kaser, G.: Indian Ocean zonal mode activity in a multicentury integration of a coupled AOGCM consistent with climate proxy data, *Geophys. Res. Lett.*, 33, 1–5, doi:10.1029/2006GL026384, 2006.

Mölg, T., Cullen, N. J., Hardy, D. R., Kaser, G., and Klok, L.: Mass balance of a slope glacier on Kilimanjaro and its sensitivity to climate, *Int. J. Climatol.*, 28, 881–892, doi:10.1002/joc.1589, 2008.

Mölg, T., Cullen, N. J., Hardy, D. R., Winkler, M., and Kaser, G.: Quantifying climate change in the tropical midtroposphere over East Africa from glacier shrinkage on Kilimanjaro, *J. Climate*, 22, 4162–4181, doi:10.1175/2009JCLI2954.1, 2009a.

Mölg, T., Cullen, N. J., and Kaser, G.: Solar radiation, cloudiness and longwave radiation over low-latitude glaciers: implications for mass-balance modelling, *J. Glaciol.*, 55, 292–302, 2009b.

Mölg, T., Chiang, J. C. H., and Cullen, N. J.: Temporal precipitation variability vs. altitude on a tropical high mountain: observations and mesoscale atmospheric modelling, *Q. J. Roy. Meteor. Soc.*, 135, 1439–1455, doi:10.1002/qj.461, 2009c.

Mölg, T., Maussion, F., Yang, W., and Scherer, D.: The footprint of Asian monsoon dynamics in the mass and energy balance of a Tibetan glacier, *The Cryosphere*, 6, 1445–1461, doi:10.5194/tc-6-1445-2012, 2012.

## Climatic controls and climate proxy potential of Lewis Glacier, Mt Kenya

R. Prinz et al.

[Title Page](#)

[Abstract](#)

[Introduction](#)

[Conclusions](#)

[References](#)

[Tables](#)

[Figures](#)

[◀](#)

[▶](#)

[◀](#)

[▶](#)

[Back](#)

[Close](#)

[Full Screen / Esc](#)

[Printer-friendly Version](#)

[Interactive Discussion](#)



Mölg, T., Cullen, N. J., Hardy, D. R., Kaser, G., Nicholson, L., Prinz, R., and Winkler, M.: East African glacier loss and climate change: corrections to the UNEP article “Africa without ice and snow”, *Environ. Dev.*, 6, 1–6, doi:10.1016/j.envdev.2013.02.001, 2013.

Mölg, T., Maussion, F., and Scherer, D.: Mid-latitude westerlies as a driver of glacier variability in monsoonal High Asia, *Nature Climate Change*, 3, 1–6, doi:10.1038/nclimate2055, 2014.

Mutai, C. C. and Ward, M. N.: East African rainfall and the tropical circulation/convection on intraseasonal to interannual timescales, *J. Climate*, 13, 3915–3939, doi:10.1175/1520-0442(2000)013<3915:EARATT>2.0.CO;2, 2000.

Nicholson, L. I., Prinz, R., Mölg, T., and Kaser, G.: Micrometeorological conditions and surface mass and energy fluxes on Lewis Glacier, Mt Kenya, in relation to other tropical glaciers, *The Cryosphere*, 7, 1205–1225, doi:10.5194/tc-7-1205-2013, 2013.

Nicholson, S. E.: A review of climate dynamics and climate variability in Eastern Africa, in: *The Limnology, Climatology and Paleoclimatology of the East African Lakes*, edited by: Johnson, T. C. and Odada, E., Gordon and Breach, Amsterdam, 25–56, 1996.

Nicholson, S. E.: An analysis of recent rainfall conditions in eastern Africa, *Int. J. Climatol.*, doi:10.1002/joc.4358, online first, 2015.

Nicholson, S. E. and Yin, X.: Rainfall conditions in Equatorial East Africa during the nineteenth century as inferred from the record of Lake Victoria, *Climatic Change*, 48, 387–398, 2001.

Niemelä, S., Räisänen, P., and Savijärvi, H.: Comparison of surface radiative flux parameterisations. Part I: Longwave radiation, *Atmos. Res.*, 58, 1–18, doi:10.1016/S0169-8095(01)00084-9, 2001.

Oerlemans, J. and Knap, W. H.: A 1 year record of global radiation and albedo in the ablation zone of Morteratschgletscher, Switzerland, *J. Glaciol.*, 44, 231–238, 1998.

Patzelt, G., Schneider, E., and Moser, G.: Der Lewis-Gletscher, Mount Kenya: Begleitworte zur Gletscherkarte 1983, *Zeitschrift für Gletscherkunde und Glazialgeologie*, 20, 177–195, 1984.

Pepin, N. C. and Lundquist, J. D.: Temperature trends at high elevations: patterns across the globe, *Geophys. Res. Lett.*, 35, 1–6, doi:10.1029/2008GL034026, 2008.

Petersen, L. and Pellicciotti, F.: Spatial and temporal variability of air temperature on a melting glacier: atmospheric controls, extrapolation methods and their effect on melt modeling, Juncal Norte Glacier, Chile, *J. Geophys. Res.*, 116, D23109, doi:10.1029/2011JD015842, 2011.

**Climatic controls and  
climate proxy  
potential of Lewis  
Glacier, Mt Kenya**

R. Prinz et al.

Title Page

Abstract

Introduction

Conclusions

References

Tables

Figures

◀

▶

◀

▶

Back

Close

Full Screen / Esc

Printer-friendly Version

Interactive Discussion



- Platt, C. M.: Some observations on the climate of Lewis Glacier, Mount Kenya, during the rainy season, *J. Glaciol.*, 6, 267–287, 1966.
- Prinz, R., Fischer, A., Nicholson, L., and Kaser, G.: Seventy-six years of mean mass balance rates derived from recent and re-evaluated ice volume measurements on tropical Lewis Glacier, Mount Kenya, *Geophys. Res. Lett.*, 38, L20502, doi:10.1029/2011GL049208, 2011.
- Prinz, R., Nicholson, L., and Kaser, G.: Variations of the Lewis Glacier, Mount Kenya, 2004–2012, *Erdkunde*, 66, 255–262, doi:10.3112/erdkunde.2012.03.05, 2012.
- Røhr, P. C. and Killingtveit, Å.: Rainfall distribution on the slopes of Mt Kilimanjaro, *Hydrolog. Sci. J.*, 48, 65–77, doi:10.1623/hysj.48.1.65.43483, 2003.
- Schneider, E.: Begleitworte zur Karte des Mount Kenya in 1 : 10000, in: *Khumbu Himal, Ergebnisse des Forschungsunternehmens Nepal Himalaya*, edited by: Hellmich, W., Springer Verlag, Berlin Göttingen Heidelberg, 20–23, 1964.
- Shea, J. M. and Moore, R. D.: Prediction of spatially distributed regional-scale fields of air temperature and vapor pressure over mountain glaciers, *J. Geophys. Res.*, 115, 1–15, doi:10.1029/2010JD014351, 2010.
- Sicart, J. E., Pomeroy, J. W., Essery, R., and Bewley, D.: Incoming longwave radiation to melting snow: observations, sensitivity, and estimation in northern environments, *Hydrol. Process.*, 20, 3697–3708, doi:10.1002/hyp.6383, 2006.
- Sicart, J. E., Hock, R., Ribstein, P., Litt, M., and Ramirez, E.: Analysis of seasonal variations in mass balance and meltwater discharge of the tropical Zongo Glacier by application of a distributed energy balance model, *J. Geophys. Res.*, 116, D13105, doi:10.1029/2010JD015105, 2011.
- Thompson, B. W.: The mean annual rainfall of Mount Kenya, *Weather*, 21, 48–49, 1966.
- Thompson, L. G. and Hastenrath, S.: Climatic ice core studies at Lewis Glacier, Mount Kenya, *Zeitschrift für Gletscherkunde und Glazialgeologie*, 17, 115–123, 1981.
- Tierney, J. E., Smerdon, J. E., Anchukaitis, K. J., and Seager, R.: Multidecadal variability in East African hydroclimate controlled by the Indian Ocean, *Nature*, 493, 389–92, doi:10.1038/nature11785, 2013.
- van den Broeke, M. R., Reijmer, C. H., van As, D., and Boot, W.: Daily cycle of the surface energy balance in Antarctica and the influence of clouds, *Int. J. Climatol.*, 26, 1587–1605, doi:10.1002/joc.1323, 2006.
- Verschuren, D., Laird, K. R., and Cumming, B. F.: Rainfall and drought in equatorial east Africa during the past 1100 years, *Nature*, 403, 410–414, 2000.



## Climatic controls and climate proxy potential of Lewis Glacier, Mt Kenya

R. Prinz et al.

Title Page

Abstract

Introduction

Conclusions

References

Tables

Figures

◀

▶

◀

▶

Back

Close

Full Screen / Esc

Printer-friendly Version

Interactive Discussion



**Table 1.** Periods of available meteorological input for cross-validation.

period	from to	number of days
1	26 September 2009–24 January 2010	121
2	2 March 2010–19 July 2010	140
3	29 September 2010–1 March 2011	154
4	2 March 2011–14 September 2011	197
5	15 September 2011–22 February 2012	161



## Climatic controls and climate proxy potential of Lewis Glacier, Mt Kenya

R. Prinz et al.

**Table 3.** Model uncertainties expressed as root mean squared error (RSME) and correlation coefficient ( $r$ ) for surface height change (sfc), daily mean surface temperature (TS) and albedo ( $\alpha$ ) at the location of the AWS.

	RSME			$r$		
	sfc [cm]	TS [°C]	$\alpha$	sfc	TS	$\alpha$
all 773 days	29.7	1.23	0.15	0.81	0.72	0.54
last 358 days (= mass balance year 2011/12)	17.2	1.03	0.09	0.78	0.78	0.83

[Title Page](#)
[Abstract](#)
[Introduction](#)
[Conclusions](#)
[References](#)
[Tables](#)
[Figures](#)




[Back](#)
[Close](#)
[Full Screen / Esc](#)
[Printer-friendly Version](#)
[Interactive Discussion](#)


## Climatic controls and climate proxy potential of Lewis Glacier, Mt Kenya

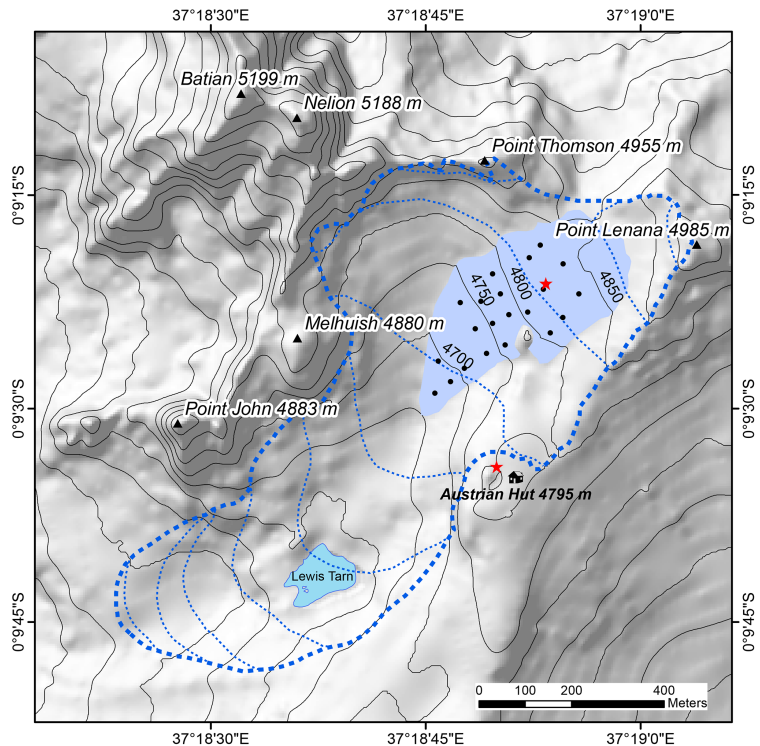
R. Prinz et al.

**Table 4.** Mean air temperature ( $T$ ), relative humidity (RH), effective cloud cover fraction ( $n_{\text{eff}}$ ), wind speed ( $v$ ), and accumulation sum for different scenarios and the 2011/12 mass balance year for different seasons: annual (wet season/dry season). Mass balance modelled under each scenario for the 2010 glacier extent is denoted by  $B$  ( $\pm 355 \text{ kg m}^{-2}$ ).

Variable (unit)	Scenarios							2011/12
	WW	CD	WET	DRY	AMPW	ATT	AMPC	REF
$T$ (°C)	-0.11 (-0.15/-0.06)	-2.11 (-2.11/-2.10)	-1.05 (-1.07/-1.03)	-0.93 (-0.92/-0.94)	-1.13 (-0.15/-2.10)	-1.09 (-2.11/-0.06)	-1.59 (-1.07/-2.10)	-1.11 (-0.96/-1.27)
RH (%)	78 (81/76)	67 (71/64)	77 (79/75)	75 (78/71)	72 (81/64)	74 (71/76)	71 (79/64)	73 (79/67)
$n_{\text{eff}}$ (%)	28 (29/27)	23 (26/21)	28 (28/27)	26 (28/24)	25 (29/21)	26 (26/27)	25 (28/21)	26 (27/26)
$v$ ( $\text{ms}^{-1}$ )	2.6 (2.6/2.7)	3.1 (2.8/3.4)	2.7 (2.7/2.7)	2.8 (2.6/2.9)	3.0 (2.6/3.4)	2.7 (2.8/2.7)	3.1 (2.7/3.4)	2.8 (2.8/2.7)
acc (cm)	355 (300/55)	152 (140/12)	349 (296/54)	188 (166/21)	312 (300/12)	195 (140/55)	308 (296/12)	232 (142/88)
$B$ ( $\text{kg m}^{-2}$ )	-527 (+580/-1107)	-578 (+115/-693)	+447 (+696/-249)	-1384 (-186/-1197)	+66 (+592/-526)	-1242 (+112/-1354)	+260 (+688/-427)	-966 (-414/-552)

[Title Page](#)
[Abstract](#)
[Introduction](#)
[Conclusions](#)
[References](#)
[Tables](#)
[Figures](#)

[Back](#)
[Close](#)
[Full Screen / Esc](#)
[Printer-friendly Version](#)
[Interactive Discussion](#)

**Figure 1.** Overview map of LG for 2010 (0.1 km<sup>2</sup>) and the late 19th century (L19, 0.6 km<sup>2</sup>, dashed). Red stars denote AWS locations, black dots the ablation stakes. L19 outline from Patzelt et al. (1984) with reconstructed contour lines. Off-glacier contours were taken from Schneider (1964) and updated for LG basin 2010 (Prinz et al., 2012).

Climatic controls and climate proxy potential of Lewis Glacier, Mt Kenya

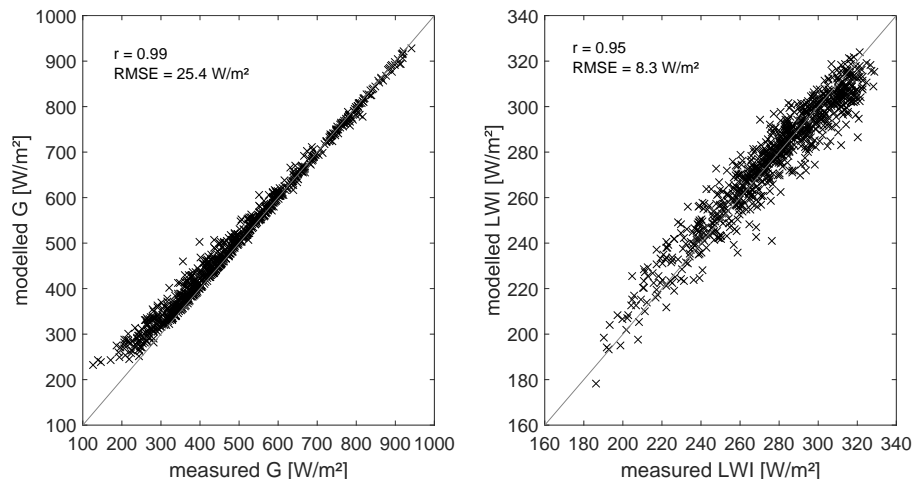
R. Prinz et al.

Title Page	
Abstract	Introduction
Conclusions	References
Tables	Figures
◀	▶
◀	▶
Back	Close
Full Screen / Esc	
Printer-friendly Version	
Interactive Discussion	



## Climatic controls and climate proxy potential of Lewis Glacier, Mt Kenya

R. Prinz et al.

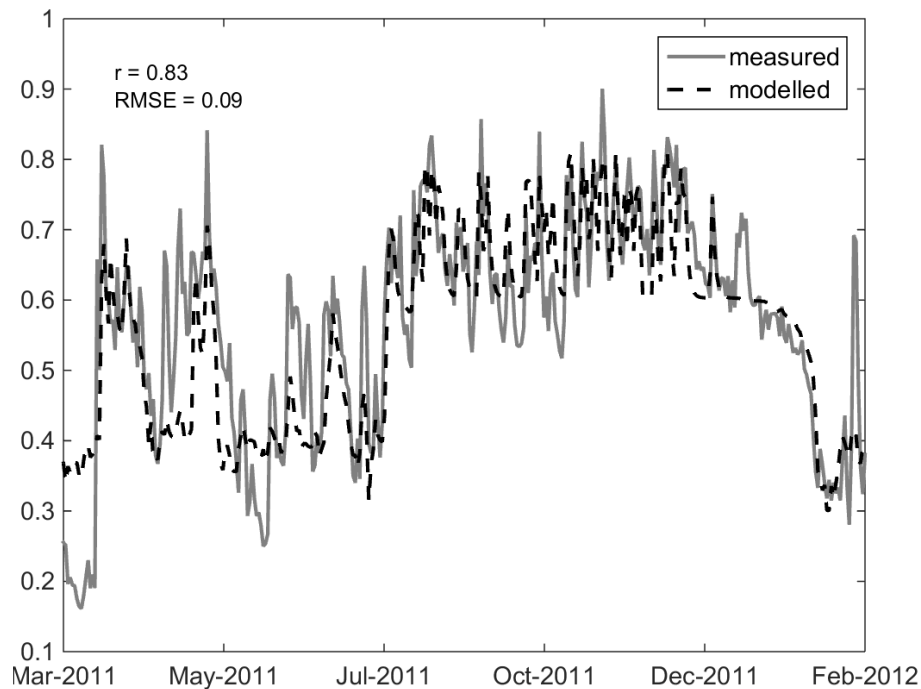


**Figure 2.** Parameterization performance of downward radiative fluxes for 772 days at the location of the AWS. Scatterplot of mean daily measured vs. modelled  $G$  (left) and  $LWI$  (right). Hourly values show similar correlation of  $r = 0.99$  ( $0.93$ ) and  $RSME = 26.4$  ( $33.8$ )  $W m^{-2}$  for  $G$  ( $LWI$ ), respectively.

[Title Page](#)[Abstract](#)[Introduction](#)[Conclusions](#)[References](#)[Tables](#)[Figures](#)[◀](#)[▶](#)[◀](#)[▶](#)[Back](#)[Close](#)[Full Screen / Esc](#)[Printer-friendly Version](#)[Interactive Discussion](#)

## Climatic controls and climate proxy potential of Lewis Glacier, Mt Kenya

R. Prinz et al.

[Title Page](#)[Abstract](#)[Introduction](#)[Conclusions](#)[References](#)[Tables](#)[Figures](#)[◀](#)[▶](#)[◀](#)[▶](#)[Back](#)[Close](#)[Full Screen / Esc](#)[Printer-friendly Version](#)[Interactive Discussion](#)

**Figure 3.** Daily mean values of measured and modelled  $\alpha$  for the 358 day mass balance year 2 March 2011 until 22 February 2012. Varying ice albedo is computed as a function of the dew point temperature (DPT):  $0.0056\text{ }^{\circ}\text{C}^{-1}$  DPT + 0.4179.

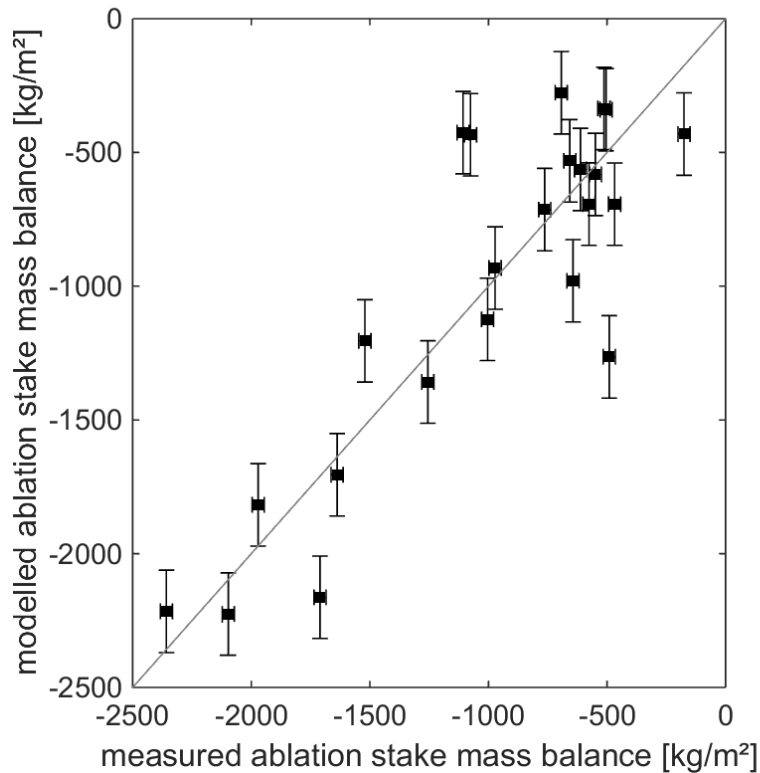


**Figure 4.** Model performance at the ablation stakes for the mass balance year 2011/12.

**Climatic controls and climate proxy potential of Lewis Glacier, Mt Kenya**

R. Prinz et al.

Title Page

Abstract Introduction

Conclusions References

Tables Figures

◀ ▶

◀ ▶

Back Close

Full Screen / Esc

Printer-friendly Version

Interactive Discussion



Climatic controls and climate proxy potential of Lewis Glacier, Mt Kenya

R. Prinz et al.

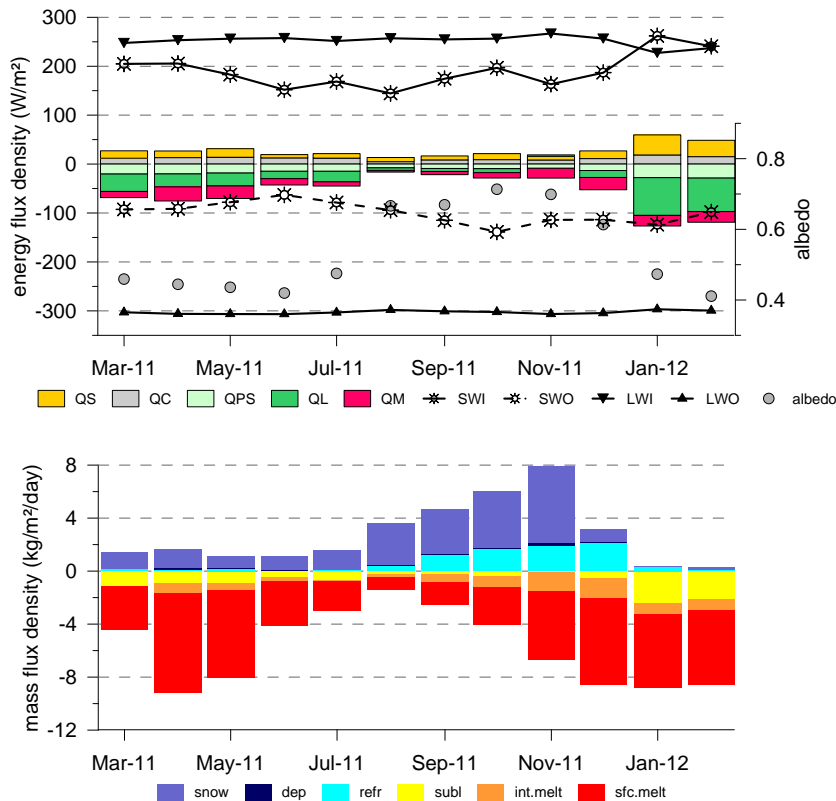


**Figure 5.** Glacier-wide mean monthly energy (upper panel) and mass flux densities (lower panel) for the mass balance year 2011/12 (REF): abbreviations as defined in Sect. 2.2 – the heat flux from precipitation is not shown due to its very low values; sfc.melt (surface melt), int.melt (internal melt in the subsurface), subl (sublimation), refr (refreezing), dep (deposition).

Title Page

Abstract

Introduction

Conclusions

References

Tables

Figures

◀

▶

◀

▶

Back

Close

Full Screen / Esc

Printer-friendly Version

Interactive Discussion



## Climatic controls and climate proxy potential of Lewis Glacier, Mt Kenya

R. Prinz et al.

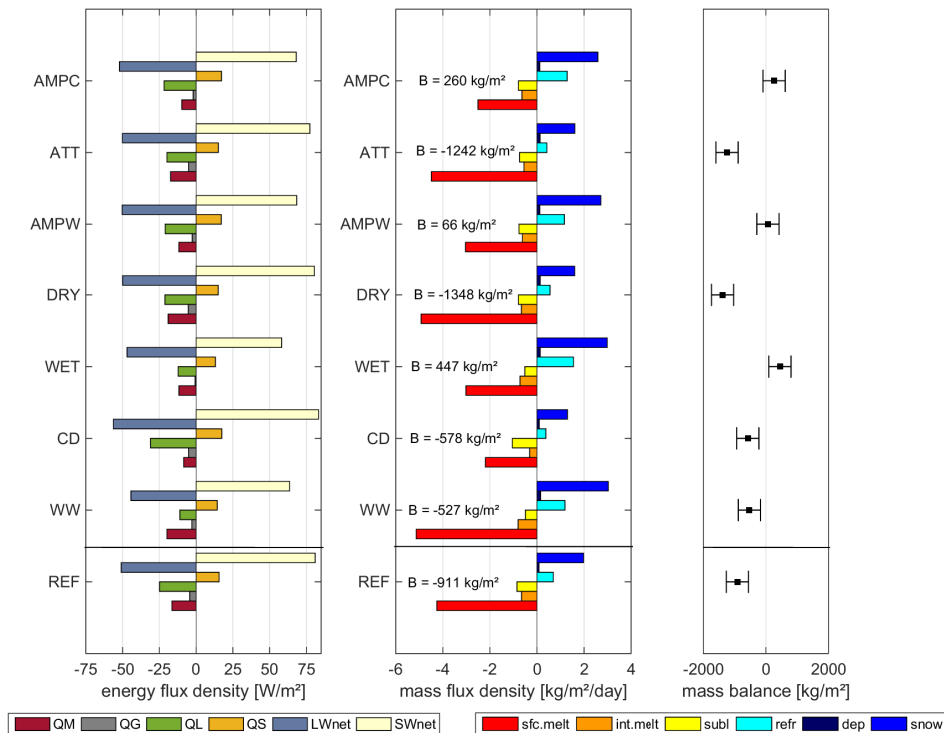


**Figure 6.** Glacier-wide mean energy (left) and mass flux densities (middle) for the eight different scenarios. The annual mass balances ( $B$ ) are shown in the middle panel and their error ranges in the right panel. Abbreviations as defined in Sect. 2.2 and Fig. 5, except QG (ground heat flux as the sum of QC and QPS), LWnet (net long-wave radiative flux), and SWnet (net short-wave radiative flux).

Title Page

Abstract Introduction

Conclusions References

Tables Figures

◀ ▶

◀ ▶

Back Close

Full Screen / Esc

Printer-friendly Version

Interactive Discussion

